

Large-Scale Energy in Turbulent Boundary Layers: Reynolds-Number and Pressure-Gradient Effects



Carlos Sanmiguel Vila, Ricardo Vinuesa, Stefano Discetti, Andrea Ianiro, Philipp Schlatter and Ramis Örlü

Abstract Adverse-pressure-gradient (APG) turbulent boundary layers (TBLs) are studied using hot-wire measurements which cover a Clauser pressure-gradient-parameter range up to $\beta \approx 2.4$. Constant and non-constant β distributions with the same upstream history are studied. The pre-multiplied power-spectral density is employed to study the differences in the large-scale energy content throughout the boundary layer. Two different large-scale phenomena are identified, the first one due to the pressure gradient and the second one due to the Reynolds number; the latter is also present in high- Re ZPG TBLs. A decomposition of the streamwise velocity fluctuations using a temporal filter shows that the small-scale velocity fluctuations do not scale in APG TBL flows since the effect of the large-scale features extends up to the near-wall region.

1 Introduction

Wall-bounded turbulent flows are one of the most fascinating and relevant problems in fluid mechanics since they appear in many relevant fluid-flow problems such as the flow around wings, land and sea vehicles, or in turbines, compressors, etc. Simplified scenarios, such as the zero-pressure-gradient (ZPG) turbulent boundary layer (TBL) developing over a flat plate, have been widely studied to understand the underlying physics of these flows [1]. Most of the engineering flows are under the effect of pressure gradients which can determine the behaviour and performance of different flow devices. Therefore, many studies are focused on extending the knowledge of TBLs under pressure-gradient effects since the applicability of the theory from ZPG TBLs to decelerating boundary layers is still rather limited. Part of the complexity associated with the study of adverse pressure gradient (APG) TBL flows is due to the

C. Sanmiguel Vila (✉) · S. Discetti · A. Ianiro
Aerospace Engineering Research Group, Carlos III University of Madrid, Leganés, Spain
e-mail: csanmigu@ing.uc3m.es

R. Vinuesa · P. Schlatter · R. Örlü
Linné FLOW Centre, KTH Mechanics, 100 44 Stockholm, Sweden
e-mail: ramis@mech.kth.se

broader parametric space with respect to their ZPG counterpart. Additional parameters associated with the influence of the pressure gradient are included in the APG studies, such as the Clauser pressure-gradient parameter, β . This quantity is defined as $\beta = (\delta^*/\tau_w)(dp/dx)$, where δ^* is the displacement thickness, τ_w is the mean wall-shear stress, and dp/dx is the pressure gradient along the streamwise coordinate. An additional difficulty is that the local state of APG TBLs is strongly affected by their streamwise history effects [2], which means that TBLs have a memory of their upstream conditions and hence need to be studied taking into account not only the local β but also the accumulated effect of β . To overcome these difficulties, it was proposed to study APG TBLs in which the value of β is maintained constant and therefore the ratio of the pressure-gradient force to the wall-shear stress remains constant [3]. From an experimental point of view, the constant β state is a challenging condition to be achieved, thus there are very few experimental studies in which a relatively large constant- β region has been achieved.

Pressure-gradient effects affect the large-scale features of the flow and increase the turbulent kinetic energy content in the outer region [4]. These findings suggest that the effects of the pressure gradient on the large-scale energy spectra appear to be similar to Reynolds number effects in ZPG turbulent boundary layers. In order to further assess the similarities and differences between both effects, new databases with an extended range of Reynolds-number and pressure-gradient conditions are needed in order to understand the individual contributions from both effects [5, 6]. With this aim in mind, different configurations of APG cases with constant β and non-constant β at matched friction Reynolds number Re_τ will be compared in order to assess the energizing effects of the APGs.

2 Experimental Setup

The experiments were performed in the Minimum Turbulence Level (MTL) closed-loop wind tunnel located at KTH Royal Institute of Technology in Stockholm. The test section is 7 m long with a cross-sectional area of $0.8 \times 1.2 \text{ m}^2$ (height \times width). The MTL is capable of reaching a maximum speed of 70 m/s with a streamwise velocity fluctuation intensity of approximately 0.025% of the free-stream velocity at a nominal speed of 25 m/s. The air temperature is controlled with an accuracy of $\pm 0.05 \text{ K}$ by means of a heat exchanger. Measurements were made in the turbulent boundary layer developing over a flat plate suspended 15 cm above the tunnel floor.

The streamwise evolution of the pressure gradient is divided into three regions: a first convergent region with a favorable pressure gradient (FPG), a second one where nearly-ZPG conditions are established and finally a divergent region where an APG is imposed, which is the region of interest for the present investigation. The different adverse-pressure-gradient conditions were obtained by changing the roof geometry in the divergent part. Modifications in the slope and shape of the divergent part allowed to obtain higher values of β by producing a stronger deceleration. The resulting pressure distributions are expressed in terms of the Clauser pressure-gradient parameter β , as shown by Fig. 1.

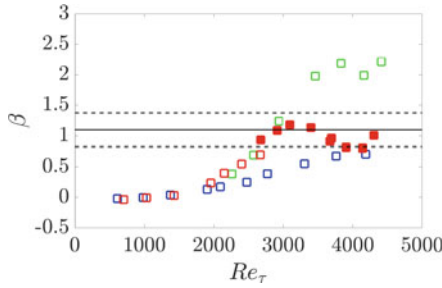


Fig. 1 Streamwise evolution of the Clauser pressure-gradient parameter β as a function of the friction Reynolds number Re_τ , where colour (red) represents configuration 1, (blue) configuration 2, and (green) configuration 3. Auxiliary reference black dash lines indicates $\beta = 1.1 \pm 25\%$. Filled symbols indicate the region bounded by 25% deviation from $\beta \approx 1.1$

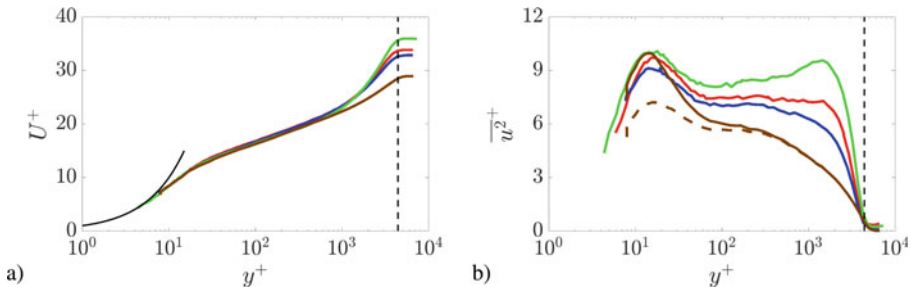


Fig. 2 Inner-scaled mean streamwise velocity (a) and streamwise variance (b), with approximately matched $Re_\tau \approx 4400$, where colour (—) represents $\beta \approx 0$ (Experimental data from Ref. [9]), (—) $\beta \approx 0.75$, (—) $\beta \approx 1.1$, and (—) $\beta \approx 2.2$. Black dashed line indicates the reference Re_τ for every case. Brown dashed line indicates raw ZPG hot-wire data without applying the correction from Ref. [10]

Single-point streamwise velocity measurements were performed by means of in-house hot-wire probes with two lengths of 525 and 275 μm and nominal diameters of 2.5 and 1.25 μm , respectively. These dimensions provided sufficient spatial resolution to ensure meaningful comparisons of the higher-order turbulence statistics. Care was taken to acquire sufficient measurement points within the viscous sublayer and the buffer region ($y^+ < 12$) in order to correct for the absolute wall position and determine the friction velocity using the composite profile reported in Ref. [7]. The correctness of the latter values were also validated against oil-film interferometry measurements at selected positions. The estimation of the 99% boundary-layer thickness δ_{99} and U_∞ was performed according to the procedure reported in Ref. [8], which is based on the diagnostic-plot concept. Using the value of δ_{99} as the upper limit of integration, δ^* and θ are obtained. With these quantities, the shape factor H_{12} and β are calculated.

3 Results and Discussion

Figure 2 shows a comparison between the inner-scaled mean velocity profiles and streamwise variance of the three APG configurations under study and a ZPG reference from Ref. [9] at matched Re_τ . Here the correction proposed in Ref. [10] is employed on the ZPG data to rectify the attenuated inner peak observed in Fig. 2 due to the large inner-scaled hot-wire length L^+ . In the outer region of the variance profiles, progressively larger values can be observed at higher β . On the other hand, for the mean velocity profiles a good collapse is observed in the inner region for all the profiles and a progressively stronger wake in the outer region as β increases. These well-known features can be connected with the scale organisation of the flow through spectral analysis. Figure 3 shows the inner-scaled pre-multiplied power-spectral density of the streamwise velocity, $f^+ \Phi_{uu}^+$, plotted in terms of the inner-scaled wall-normal position, y^+ , and the inner-scaled time, t^+ . The overall shape of the near-wall region is relatively similar in all the configurations for both ZPG and APG. This energy distribution is connected with the inner peak which can be observed at $y^+ \approx 15$ in the streamwise variance profiles from Fig. 2 and approximately corresponds to a streamwise wavelength of $\lambda_x^+ \approx 1000$. This inner peak represents the footprint of the near-wall structure of elongated high- and low-speed regions. It should be recalled that the attenuated values in the near-wall peak at higher Re in the ZPG case, is an artifact of spatial resolution effects [11], which are not corrected for in the spectra as opposed to the variance profile. The main differences between the APG and ZPG configurations emerge when the power spectral density contours are compared for $y^+ > 100$; starting from that location the activity in all the APG configurations is more intense, especially for higher values of β . This behaviour is reflected in the onset of the outer spectral peak in the APG cases, which is in good agreement with the characteristic peak reported in previous studies [2, 4, 6]. This outer peak is approximately located at $y/\delta^* = 1$, an observation connected with the results from Kitsios et al. [12] in which the maxima of the Reynolds stresses are reported at approximately that location. Apart from this outer peak, in the high- Re cases an additional region of high energy density emerges, for both ZPG and APG configurations. This second outer spectral peak is located at the middle of the logarithmic region, $y^+ \approx 3.9Re_\tau^{0.5}$, and is associated with the large-scale motions which were also observed in ZPG configurations at high Re_τ [13]. This effect appears to be independent of the pressure gradient and is associated with phenomena which have longer t periods than those associated with the APG outer spectral peak [4]. In contrast with the observations made by Harun et al. [4], who suggested that this peak is overshadowed by the presence of the structures with longer periods, here we show that at high Reynolds numbers both effects are present. Analysing the different configurations, it is observed that larger values of β are connected to larger power-spectral density, which confirms that larger values of β increase the population of large-scale motions as suggested by Harun et al. [4]. The effect of the interaction between the different scales and their effect on the Reynolds stresses is quantified via a scale-decomposition analysis with a cut-off period equal to $t^+ = 400$. This value is a reasonable compromise to

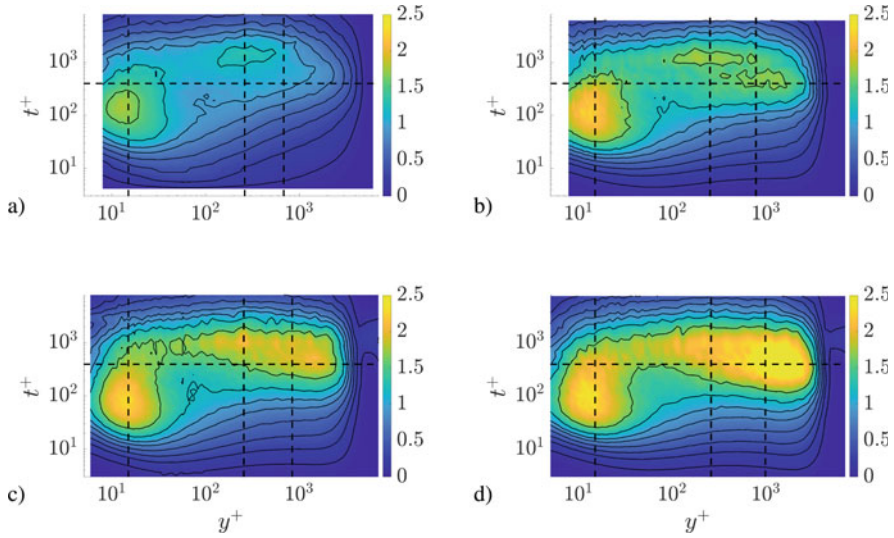
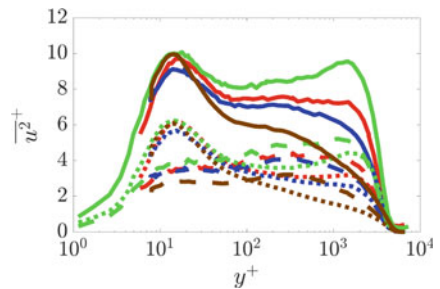


Fig. 3 Inner-scaled premultiplied energy spectra of the streamwise velocity at $Re_\tau \approx 4400$ with contour levels at $f^+ \Phi_{uu}^+ = 0.1, 0.25, 0.4, 0.575, 0.775, 0.95, 1.2, 1.6, 2.0$. (a) $\beta \approx 0$ (Experimental data from Ref. [9]), (b) $\beta \approx 0.75$, (c) $\beta \approx 1.1$, (d) $\beta \approx 2.2$. Auxiliary vertical dashed lines are located at $y^+ = 15$, $y^+ = 3.9Re_\tau^{0.5}$ and $y/\delta^* = 1$. Auxiliary horizontal dashed line is placed at $t^+ = 400$

Fig. 4 Decomposition of the velocity fluctuations (solid lines) into a small-scale (dotted lines) and a large-scale (dashed lines) component for $Re_\tau \approx 4400$. Colour (—) represents $\beta \approx 0$, (—) $\beta \approx 0.75$, (—) $\beta \approx 1.1$, and (—) $\beta \approx 2.2$



effectively separate small- and large-scale components of the streamwise velocity fluctuations. Figure 4 shows the small- and large-scale variance of the streamwise velocity fluctuations. It is observed that with increasing pressure-gradient strength the penetration of the large-scale components toward the near-wall region increases. While the small-scale energy in ZPGs scales throughout the entire boundary-layer thickness, it is clear that this does not extend to APG TBLs, where the small-scale energy contribution is also enhanced in the outer region, where spatial resolution effects are not to be expected [11]. This has a clear impact on the correction schemes for spatial resolution effects that consider the viscous length-scale as the governing parameter [10], since these schemes should thus be employed with caution for APG TBLs.

Acknowledgements CSV acknowledges the financial support from Universidad Carlos III de Madrid within the program “Ayudas para la Movilidad del Programa Propio de Investigación”. RÖ, RV and PS acknowledge the financial support from the Swedish Research Council (VR) and the Knut and Alice Wallenberg (KAW) Foundation as part of the Wallenberg Academy Fellow programme. CSV, SD and AI were partially supported by the Grant DPI2016-79401-R funded by the Spanish State Research Agency (SRA) and European Regional Development Fund (ERDF).

References

1. P. Schlatter, R. Örlü, Assessment of direct numerical simulation data of turbulent boundary layers. *J. Fluid Mech.* **659**, 116–126 (2010)
2. A. Bobke, R. Vinuesa, R. Örlü, P. Schlatter, History effects and near equilibrium in adverse-pressure-gradient turbulent boundary layers. *J. Fluid Mech.* **820**, 667–692 (2017)
3. F.H. Clauser, Turbulent boundary layers in adverse pressure gradients. *J. Aero Sci* **21**, 91–108 (1954)
4. Z. Harun, J.P. Monty, R. Mathis, I. Marusic, Pressure gradient effects on the large-scale structure of turbulent boundary layers. *J. Fluid Mech.* **715**, 477–498 (2013)
5. R. Vinuesa, R. Örlü, C. Sanmiguel Vila, A. Ianiro, S. Discetti, P. Schlatter, Revisiting history effects in adverse-pressure-gradient turbulent boundary layers. *Flow Turbul. Combust.* **99**, 565–587 (2017)
6. C. Sanmiguel Vila, R. Örlü, R. Vinuesa, P. Schlatter, A. Ianiro, S. Discetti, Adverse-pressure-gradient effects on turbulent boundary layers: statistics and flow-field organization. *Flow Turbul. Combust.* **99**, 589–612 (2017)
7. K.A. Chauhan, P.A. Monkewitz, H.M. Nagib, Criteria for assessing experiments in zero pressure gradient boundary layers. *Fluid Dyn. Res.* **41**, 021404 (2009)
8. R. Vinuesa, A. Bobke, R. Örlü, P. Schlatter, On determining characteristic length scales in pressure-gradient turbulent boundary layers. *Phys. Fluids* **28**, 055101 (2016)
9. R. Örlü, Experimental studies in jet flows and zero pressure-gradient turbulent boundary layers. Ph. D. thesis, Royal Institute of Technology (2009)
10. A.J. Smits, J.P. Monty, M. Hultmark, S.C.C. Bailey, N. Hutchins, I. Marusic, Spatial resolution correction for wall-bounded turbulence measurements. *J. Fluid Mech.* **676**, 41–53 (2011)
11. N. Hutchins, T.B. Nickels, I. Marusic, M.S. Chong, Hot-wire spatial resolution issues in wall-bounded turbulence. *J. Fluid Mech.* **635**, 103–136 (2009)
12. V. Kitsios, A. Sekimoto, C. Atkinson, J.A. Sillero, G. Borrell, A.G. Gungor, J. Jiménez, J. Soria, Direct numerical simulation of a self-similar adverse pressure gradient turbulent boundary layer at the verge of separation. *J. Fluid Mech.* **829**, 392–419 (2017)
13. N. Hutchins, I. Marusic, Evidence of very long meandering features in the logarithmic region of turbulent boundary layers. *J. Fluid Mech.* **579**, 1–28 (2007)